Brain, Behavior, and Immunity 57 (2016) 106–115

Contents lists available at ScienceDirect

Brain, Behavior, and Immunity

journal homepage: www.elsevier.com/locate/ybrbi

Full-length Article

# $\beta_2$-Adrenoceptors on tumor cells play a critical role in stress-enhanced metastasis in a mouse model of breast cancer

Aeson Chang [a], Caroline P. Le [a], Adam K. Walker [a], Sarah J. Creed [a], Cindy K. Pon [a], Sabine Albold [a], Dominic Carroll [a], Michelle L. Halls [a], J. Robert Lane [a], Bernhard Riedel [b], Davide Ferrari [c], Erica K. Sloan [a,b,d,*]

[a] Drug Discovery Biology Theme, Monash Institute of Pharmaceutical Sciences, Monash University, Parkville, Victoria 3052, Australia
[b] Division of Cancer Surgery, Peter MacCallum Cancer Centre, East Melbourne, Victoria 3002, Australia
[c] School of Mathematics and Statistics, The University of Melbourne, Parkville, Victoria 3010, Australia
[d] Cousins Center for PNI, UCLA Semel Institute, Jonsson Comprehensive Cancer Center, and UCLA AIDS Institute, University of California Los Angeles, Los Angeles, CA 90095, USA

ARTICLE INFO

*Article history:*
Received 13 April 2016
Received in revised form 9 June 2016
Accepted 15 June 2016
Available online 16 June 2016

*Keywords:*
Breast cancer
$\beta_2$-Adrenoceptor
Chronic stress
Metastasis
Invasion

ABSTRACT

Chronic stress accelerates metastasis – the main cause of death in cancer patients – through the activation of β-adrenoceptors (βARs). We have previously shown that $\beta_2$AR signaling in MDA-MB-231$^{HM}$ breast cancer cells, facilitates invadopodia formation and invasion *in vitro*. However, in the tumor microenvironment where many stromal cells also express βAR, the role of $\beta_2$AR signaling in tumor cells in metastasis is unclear. Therefore, to investigate the contribution of $\beta_2$AR signaling in tumor cells to metastasis *in vivo*, we used RNA interference to generate MDA-MB-231$^{HM}$ breast cancer cells that are deficient in $\beta_2$AR. $\beta_2$AR knockdown in tumor cells reduced the proportion of cells with a mesenchymal-like morphology and, as expected, reduced tumor cell invasion *in vitro*. Conversely, overexpression of $\beta_2$AR in low metastatic MCF-7 breast cancer cells induced an invasive phenotype. Importantly, we found that knockdown of $\beta_2$AR in tumor cells significantly reduced the impact of stress on metastasis *in vivo*. These findings highlight a crucial role for $\beta_2$AR tumor cell signaling in the adverse effects of stress on metastasis, and indicate that it may be necessary to block $\beta_2$AR on tumor cells to fully control metastatic progression.


## 1. Introduction

Despite advances in cancer treatment, metastasis remains the greatest clinical challenge in the management of cancer and contributes to the majority of deaths in cancer patients (Mehlen and Puisieux, 2006). Studies have revealed that chronic stress drives cancer progression by accelerating metastasis in *in vivo* mouse models of various cancer types (Ben-Eliyahu et al., 2000; Campbell et al., 2012; Kim-Fuchs et al., 2014; Lamkin et al., 2015; Le et al., 2016; Liu et al., 2015; Sloan et al., 2010; Thaker et al., 2006; Zhao et al., 2015). This raises the possibility that targeting stress responsive signaling may help slow cancer progression and metastatic dissemination (Sloan et al., 2010; Thaker et al., 2006), and provide a much needed additional therapy for the treatment of cancer.

The sympathetic nervous system (SNS) plays an important role in the response to stress, which triggers the release of catecholaminergic neurotransmitters from SNS nerve fibers (Elenkov et al., 2000). These neurotransmitters activate β-adrenoceptors (βARs), which induces downstream signaling in responsive cells and leads to transcriptional changes (Elenkov et al., 2000). A number of different cell types present within the tumor microenvironment express βARs, and thus are able to respond to stress signaling. These include immune cells and endothelial cells (Abrass et al., 1985; Graf et al., 1993; Sanders et al., 1997), which have a critical role in driving cancer progression (Condeelis and Pollard, 2006; Folkman, 2002; Le et al., 2016). In response to stress, stromal cells contribute to metastasis by remodeling tumor architecture in ways that favor dissemination of tumor cells. This includes macrophage recruitment into the primary tumor (Sloan et al., 2010; Zhao et al., 2015) and vascular remodeling to increase blood vessel (Sloan et al., 2010; Thaker et al., 2006) and lymph vessel (Le et al., 2016) routes of tumor cell dissemination. Experimental strategies that prevent either macrophage recruitment or vascular remodeling block stress-enhanced metastasis (Le et al., 2016; Sloan et al., 2010; Thaker et al., 2006), demonstrating that regulation of the tumor stroma plays an important role in the effects of stress on cancer progression.

Tumor cells also express βARs (Pon et al., 2016; Reeder et al., 2015), and activation of βAR signaling increases invasion of tumor cells, as measured by *in vitro* assays (Creed et al., 2015; Kim-Fuchs

* Corresponding author at: 381 Royal Parade, Parkville, Victoria 3052, Australia.
*E-mail address:* erica.sloan@monash.edu (E.K. Sloan).

http://dx.doi.org/10.1016/j.bbi.2016.06.011
0889-1591/

et al., 2014; Pon et al., 2016; Yamazaki et al., 2014) and in explant cultures (Creed et al., 2015). Previously, we discovered that the $\beta_2$AR-selective agonist formoterol, but not the $\beta_1$AR-selective agonist xamoterol, induced the formation of invadopodia in breast cancer cells (Creed et al., 2015). Invadopodia are actin-rich cellular structures that localize matrix metalloproteases (MMPs) and degrade the extracellular matrix for tumor cell invasion (Murphy and Courtneidge, 2011). However, the role of $\beta_2$AR-regulated invasion *in vivo* is less clear. Unlike in simple *in vitro* assays, in the tumor microenvironment contextual cues provided by stromal cells influence whether tumor cells are able to escape the primary tumor and disseminate to distant tissues (Bissell and Labarge, 2005; Devaud et al., 2014). Therefore, in the complex tumor microenvironment where stromal cells also respond to βAR stress signaling, it is unclear whether $\beta_2$AR signaling in tumor cells significantly contributes to metastasis. Previous studies that used systemic β-blockade to investigate βAR regulation of metastasis were unable to distinguish the contribution of βAR signaling in tumor cells, as systemic β-blockade indiscriminately targets both tumor cells and stromal cells (Campbell et al., 2012; Sloan et al., 2010; Thaker et al., 2006). While use of siRNA has shown that $\beta_2$AR signaling affects the growth of tumor cells injected directly into metastatic target organs (Thaker et al., 2006), it is not known if signaling from $\beta_2$ARs on tumor cells is required for the early stages of the metastatic cascade including tumor cell invasion and escape from the primary tumor.

To address this, we used an shRNA approach to generate breast cancer cells that were stably deficient in $\beta_2$AR. Using MDA-MB-231$^{HM}$ cells, a human breast cancer cell line that is highly responsive to βAR signaling, we investigated the effect of tumor cell $\beta_2$AR knockdown on metastasis from a primary orthotopic mammary tumor. Consistent with previous pharmacologic studies, genetic modulation of MDA-MB-231$^{HM}$ $\beta_2$AR reduced cell invasion, and prevented a shift to mesenchymal cell morphology. Conversely, upregulating $\beta_2$AR expression in MCF-7 tumor cells with low endogenous $\beta_2$AR expression increased invadopodia formation, demonstrating a central role for $\beta_2$AR in regulating tumor cell invasion. Furthermore, we show that $\beta_2$AR modulation in MDA-MB-231$^{HM}$ tumor cells attenuated stress-enhanced metastasis from primary mammary tumors. These findings show that in this model of breast cancer, $\beta_2$AR-driven tumor cell invasion plays a significant role in the effects of stress on metastasis. These findings suggest that pharmacological strategies that block the effects of stress on metastasis may need to also target $\beta_2$AR on tumor cells to fully control metastatic progression.

## 2. Methods

### 2.1. Genetic manipulation of tumor cell $\beta_2$AR expression

The human breast cancer cell line MDA-MB-231$^{HM}$ (a kind gift from Dr. Zhou Ou, Fudan University Shanghai Cancer Center, China) (Chang et al., 2008) was transduced with a lentiviral vector containing codon optimized firefly luciferase under the control of the ubiquitin-C promoter as previously described (Le et al., 2016). The identity of the cell line was confirmed by karyotyping (CellBank Australia). Cells were maintained in DMEM (Invitrogen, USA) supplemented with 200 mM glutamine and 10% fetal bovine serum (FBS; Life Technologies, USA) at 37 °C with 5% $CO_2$. To silence *ADRB2,* cells were transduced with shRNA that specifically targets human *ADRB2* (shADRB2a: 5′-TGCTGTGACTTCTTCACGA-3′; shADRB2b: 5′-GCCATCAACTGCTATGCCA-3′) or scramble control sequence (SCR): 5′-ATCTCGCTTGGGCGAGAGTAAG-3′ (Dharmacon, USA). MCF-7 cells were acquired from ATCC (Manassas, Virginia) and grown in MEM supplemented with 200 mM glutamine and 10% FBS. The $\beta_2$AR-GFP construct was made by sub-cloning the human $\beta_2$AR coding sequence 5′ to a codon-humanized GFP gene derived from the vector pGFP$^2$-N1 (Perkin Elmer), and sequence verified. Cells were stably transduced and GFP-positive cells sorted by FACS. All experiments used bulk cell populations to avoid clonal effects. Cells were confirmed negative for mycoplasma using MycoAlert™ Mycoplasma Detection Kit (Lonza, Australia).

### 2.2. Functional analysis of $\beta_2$AR knockdown in tumor cells by cAMP accumulation assay

Tumor cells ($4 \times 10^4$) were seeded into a 96-well plate and serum-starved overnight. Cells were then washed and incubated in pre-warmed stimulation buffer (140 mM NaCl, 5 mM KCl, 800 nM $MgSO_4$, 200 nM $Na_2HPO_4$, 440 nM $KH_2PO_4$, 5 mM HEPES, 1.3 mM $CaCl_2$, 5.6 mM glucose, 0.1% w/v BSA, 500 μM 3-isobutyl-1-methylxanthine, pH 7.4) at 37 °C in 0% $CO_2$ for 30 min. Formoterol hemifumarate ($\beta_2$AR-selective agonist; Tocris, UK) at indicated concentrations was then added for 10 min before cells were lysed with ice-cold 100% ethanol, evaporated and rehydrated with 50 μL detection buffer (0.1% BSA, 5 mM HEPES, 0.3% Tween20, pH 7.4). cAMP in cell lysates (5 μL) was then incubated with 1 unit of AlphaScreen™ acceptor beads (Perkin Elmer, USA) diluted in detection buffer, followed by incubation with 1 unit of donor beads. Fluorescence signal was measured using a Fusion plate reader (Perkin Elmer, USA). cAMP accumulation was expressed as pmol/well.

### 2.3. Tumor cell proliferation

Tumor cells ($5 \times 10^4$) were seeded into a 12 well plate and serum-starved overnight. Cells were then treated with 1 μM isoproterenol (non-selective β-agonist Sigma, USA) in vehicle (DMEM supplemented with 2% FBS). Isoproterenol was replenished every 24 h. Cell numbers were quantified using the Tali™ Image-Based Cytometer (Invitrogen, USA) at indicated time points.

### 2.4. Cell morphology assay

Tumor cells ($5 \times 10^3$) were seeded into a 96 well plate and serum-starved overnight. Cells were then treated with or without 1 μM isoproterenol in the absence or presence of ICI-118,551 ($\beta_2$AR-selective antagonist, 1 μM, Tocris, UK) in DMEM supplemented with 2% FBS. Isoproterenol and ICI-118,551 were replaced every 24 h to minimize possible effects of auto-oxidation. Cells were imaged using a 20x long WD objective every 24 h for 3 days using the Operetta High-Content Imaging System (Perkin Elmer, USA). At each time point, nine random fields of view from each well were captured and analyzed using Harmony® High Content Imaging and Analysis Software (version 3.5, Perkin Elmer). The roundness of individual cells was assessed using the proprietary analytical tools provided in the Harmony Analysis software. The cell roundness parameter ranged between 0 and 1 where a value of 1 is equivalent to perfect roundness. The parameter threshold to define a mesenchymal-like cell was set at 0.5 (Ren et al., 2015; Yang and Weinberg, 2008). The proportion of mesenchymal-like tumor cells in the population meeting this criterion was then quantified.

### 2.5. Invadopodia assay

Gelatin was labeled with Alexa Fluor-568 protein labeling kit according to the manufacturer instructions (Life Technologies, USA). Culture vessels were coated with an 8:1 ratio of unlabeled to labeled 0.2% gelatin and topped with a thin layer of unlabeled 10 μg/mL human fibronectin to promote cell adherence.

MCF7-WT or MCF7-$\beta_2$AR cells were serum-starved overnight. Cells were then seeded onto the prepared cultured vessels containing 10% serum, ±βAR agonists (0.5 μM isoproterenol or 0.5 μM formoterol hemifumarate) for 5 h. Cells were then fixed in 4% paraformaldehyde, actin stained with phalloidin and nuclei counterstained with 1 μg/ml Hoechst 33242. Invadopodia were imaged on a Leica SP8 Confocal using a 63x PL APO CS2 1.4NA objective. Images were captured through LAS AF software version 3.2 (Leica Microsystems, North Ryde Australia). Images were prepared as Tiff stacks for actin and gelatin using ImageJ and submitted to the Invadopodia Analysis Server (IAS) and analyzed as previously described (Creed et al., 2015).

### 2.6. Gene expression analysis

Tumor cells ($7 \times 10^5$) were seeded into a 6 well plate and serum-starved overnight before treatment with vehicle, isoproterenol (1 μM), and/or ICI-118,551 ($\beta_2$AR-selective antagonist, 1 μM) in DMEM supplemented with 2% FBS for the time indicated, prior to analysis. Total RNA was isolated using RNeasy Mini Kit (Qiagen, Germany). qRT-PCR was used to quantify gene expression in 100 ng of total RNA using Taqman probes (Applied Biosystems, USA) targeting human βAR subtypes (*ADRB1* Hs02330048_s1, *ADRB2* Hs00240532_s1, *ADRB3* Hs00609046_m1) and MMP2 (*MMP2* Hs01548727_m1) and iScript One-Step RT-PCR kit (Biorad, USA) with 50 PCR amplification cycles of 15 s of strand separation at 95 °C and 30 s of annealing and extension at 60 °C. Transcript levels for genes of interest were normalized relative to scramble control cells.

### 2.7. Tumor cell invasion assay

Serum-starved tumor cells ($1.5 \times 10^5$) were suspended in 300 μL DMEM supplemented with 2% FBS with or without 1 μM isoproterenol and seeded into Transwell® chambers (8 μm pores, PET membrane, Sigma, USA) that were pre-coated with 100 μL Matrigel (2 mg/mL, BD, USA). For 24 h, cells were allowed to invade toward the bottom chamber, which was filled with media supplemented with 10% FBS with or without 1 μM isoproterenol. Membranes were then fixed with 4% paraformaldehyde (Sigma, USA) and stained with Hoechst 33342 (1:1000, Sigma, USA) and imaged using a Nikon Ti-E microscope, fitted with 10x Plan Apo 0.3NA objective and a Photometrics CoolSNAP Myo camera. Fluorescent excitation and emission was provided by a Nikon UV-A filter cube (excitation 355/50 and emission 420LP). Images were captured using NIS Elements software (version 4.3, Nikon Instruments). Invaded cells were counted using the Fiji distribution of ImageJ (Schindelin et al., 2012).

### 2.8. Breast cancer model with restraint stress

To investigate spontaneous metastasis from an orthotopic primary tumor, $2 \times 10^5$ tumor cells in 20 μL PBS (Invitrogen, USA) were injected into the left 4th mammary fat pad of anesthetized (3% isoflurane) 8 week-old female BALB/c *nu*/*nu* mice (University of Adelaide, Australia). Mice were housed under PC2 barrier conditions (temperature and humidity controlled, 12 h dark/light cycle) and acclimatized in a home cage for a week prior to tumor cell inoculation. Primary tumors were monitored by digital caliper twice a week and volume calculated using the formula: $(\text{length} \times \text{width}^2)/2$. Mice were randomly assigned to either stress or non-stress group (n = 5 per group). To induce chronic stress, mice were subjected to a well-characterized restraint stress paradigm (Sloan et al., 2010; Le et al., 2016; Thaker et al., 2006). Mice were placed in a ventilated Perspex chamber that restricted movement for 2 h per day for a total of 21 days, commencing 7 days before tumor cell injection. Mice in the non-stress group remained in their home cage throughout the 2 h period. Distant metastasis to lymph nodes and lung was monitored longitudinally twice weekly using bioluminescence imaging, which allows repeated measure analysis of metastatic burden in the same mouse throughout the experiment. Mice were injected with D-luciferin (150 mg/kg, CHOICE Analytical) via tail vein and imaged using an IVIS Lumina II (Perkin Elmer) (Le et al., 2016; Sloan et al., 2010). Mice were euthanized 28 days after tumor cell injection and tissue-specific metastasis was confirmed in lung and axillary lymph node by *ex vivo* bioluminescence imaging. *In vivo* experiments were conducted in duplicate. All procedures involving mice were carried out under protocols approved by the Institutional Animal Ethics Committee and in accordance with National Health and Medical Research Council animal ethics guidelines.

### 2.9. Statistical analysis

Longitudinal mixed-effect linear models were used to determine the effect of stress on the trajectory of metastasis, and to evaluate if those effects were modified by tumor $\beta_2$AR knockdown (Verbeke and Molenberghs, 2009). We examined the stress x treatment (tumor cell $\beta_2$AR knockdown) interaction in a 2 (non-stress vs. stress) × 3 (scramble control vs. shADRB2a vs. shADRB2b) experimental design. Data were analyzed according to the model $Y_{ijt} = \beta_1 d_{i1} t_{ij} + \beta_2 d_{i2} t_{ij} + \beta_3 d_{i3} t_{ij} + \beta_4 d_{i4} t_{ij} + \beta_5 d_{i5} t_{ij} + \beta_6 d_{i6} t_{ij} + \varepsilon_{ij}$, where: $Y_{ijt}$ are mouse-specific and day-specific primary tumor volume or luciferase signals (Fig. 4a) for the ith mouse on the logarithmic scale; $t_{ij}$ is the time (days of follow up), $d_{ij}$ (j = 1,. . .,6) are binary variables so that $d_{ij} = 1$ if the ith mouse belongs to the jth group and 0 otherwise; $\varepsilon_{ij}$ is the random error term. Linear models were fitted using the routine lm while multiple comparisons used the routine glht in the package multicomp (Bretz et al., 2010). The effect of stress on the trajectory of metastasis or primary tumor volume was calculated using the difference in gradient of fitted lines between stress and non-stress conditions for each tumor cell type. Pearson's correlation analysis was performed to assess the relationship between the effect of stress on the trajectory of primary tumor volume and the effect of stress on the trajectory of metastasis. For *ADRB* expression in MCF7-WT and MCF7-$\beta_2$AR cells, unpaired t-tests were used to compare each βAR subtype between the two cell lines. For cell proliferation and cell morphology assays, the effect of isoproterenol on cell proliferation or mesenchymal-like morphology of each cell lines was compared using one-way ANOVA repeated measures followed *post hoc* Tukey's planned comparison tests when applicable. For all other experiments, a two-way ANOVA test was first performed to identify the presence of interaction between treatments. *Post hoc* Tukey's planned comparison tests were performed when applicable, to test the simultaneous differences between pairs of treatment effects on experimental responses (*MMP2* gene expression, *in vitro* invasion, number of invadopodia, *ex vivo* bioluminescence signals and primary tumor mass). Experiments were repeated 2–4 times. Treatment effects showing *p*-values smaller than 0.05 were regarded as statistically significant. Statistical analyses were carried out in both R computing environment (Team, 2014) and Prism 6 software (GraphPad Software, La Jolla, CA, USA).

## 3. Results

### 3.1. Generation of MDA-MB-231$^{HM}$ cells deficient in $\beta_2$AR

We have previously shown that $\beta_2$AR is the only functional βAR subtype in MDA-MB-231$^{HM}$ cells (Pon et al., 2016). Therefore, we used two different hairpin sequences that target the gene encoding

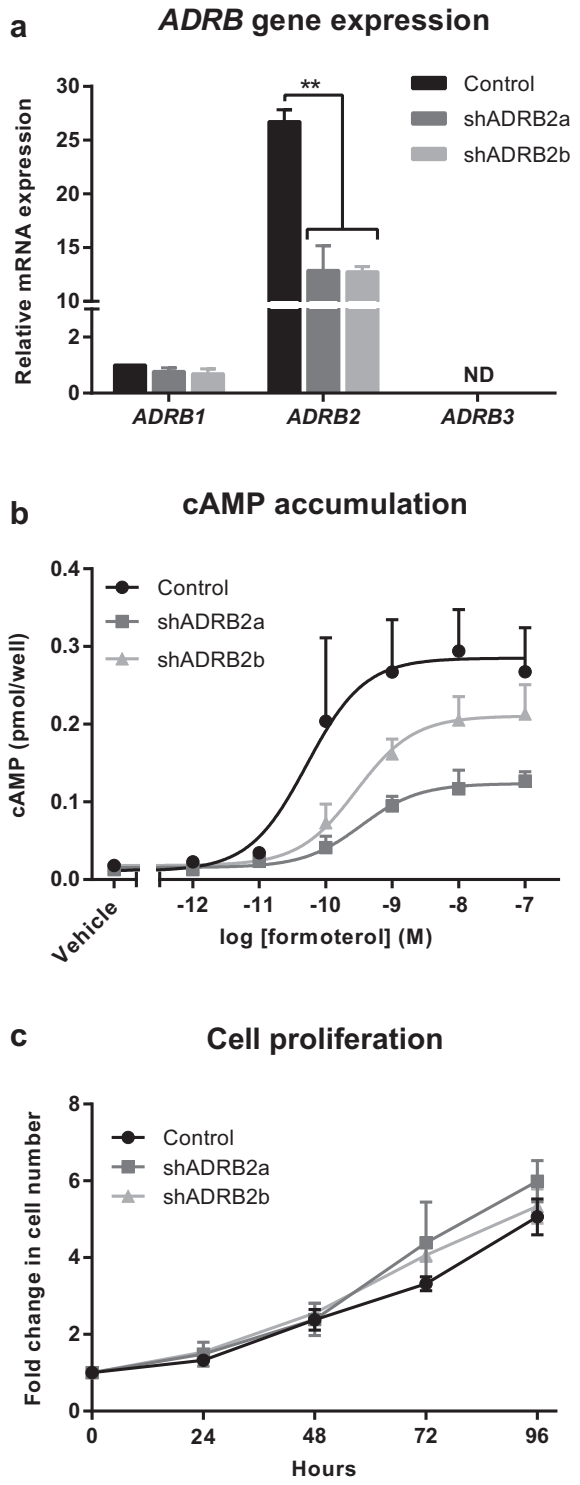


**Fig. 1. Generation of MDA-MB-231$^{HM}$ breast cancer cells deficient in $\beta_2$AR.** (a) Quantification of *ADRB* mRNA transcript levels using qRT-PCR in MDA-MB-231$^{HM}$ cells transduced with shRNA scramble sequence (control) or shRNA targeting *ADRB2* (shADRB2a and shADRB2b) (n = 4). ND: not detected. (b) Quantification of cAMP accumulation in scramble control, shADRB2a and shADRB2b tumor cells in response to increasing concentrations of the $\beta_2$AR selective-agonist formoterol (n = 3). (c) Proliferation of control, shADRB2a and shADRB2b tumor cells (n = 3). Data represent mean ± standard error. $^{**}p < 0.01$ by one-way ANOVA with *post hoc* Tukey's planned comparison tests.

$\beta_2$AR (*ADRB2*) to knock down expression of $\beta_2$AR in MDA-MB-231$^{HM}$ breast cancer cells, and generated shADRB2a and shADRB2b cell lines. To examine the efficiency of *ADRB2* silencing, we used qRT-PCR to quantify the expression of *ADRB2* in shADRB2a and shADRB2b cells relative to control cells transduced with a scrambled shRNA sequence (scramble control). *ADRB2* expression was reduced by >50% in both shADRB2a and shADRB2b cells compared to scramble control cells ($p < 0.01$) (Fig. 1a). *ADRB1* expression was not affected by shRNA transduction, and *ADRB3* expression was not detected in these cell lines (Fig. 1a), consistent with our previous findings (Creed et al., 2015; Pon et al., 2016). Stable knockdown was confirmed with reduction of the *ADRB2* transcript maintained even after 6 weeks in culture (data not shown).

To investigate the effect of *ADRB2* knockdown on receptor function, we evaluated cAMP accumulation as an indicator of receptor signaling. Cells were stimulated with the $\beta_2$AR-selective agonist formoterol, which induced cAMP accumulation in scramble control cells ($E_{max}$ = 0.29 ± 0.06 pmol/well) (Fig. 1b). However, the cAMP response was blunted in $\beta_2$AR-deficient cell lines (shADRB2a: $E_{max}$ = 0.13 ± 0.02 pmol/well; shADRB2b: $E_{max}$ = 0.21 ± 0.04 pmol/well) (Fig. 1b). Reduction of the cAMP response in $\beta_2$AR-deficient cell lines was also demonstrated by a need for a greater concentration of formoterol to reach the $EC_{50}$ (50% of the maximal response, control cells: 13.30 ± 9.25 nM vs. shADRB2a: 63.94 ± 38.67 nM; shADRB2b: 32.58 ± 13.21 nM) (Fig. 1b).

To determine if *ADRB2* knockdown affected tumor cell proliferation, we compared the *in vitro* proliferative activity of $\beta_2$AR-deficient cells to scramble control cells. $\beta_2$AR knockdown did not modulate the proliferation of tumor cells, either under baseline conditions (Fig. 1c), or after treatment with the non-selective βAR agonist isoproterenol (Supplementary Fig. 1). Collectively, these findings confirmed the generation of MDA-MB-231$^{HM}$ tumor cell lines with reduced levels of *ADRB2* transcription, blunted $\beta_2$AR signaling, and without compromised tumor cell proliferative capability.

### 3.2. Characterization of tumor cell invasiveness in MDA-MB-231$^{HM}$ cells deficient in $\beta_2$AR

Our previous studies using pharmacological modulation of $\beta_2$AR found a crucial role for tumor cell $\beta_2$AR signaling in promoting invadopodia formation and tumor cell invasion (Creed et al., 2015; Pon et al., 2016). To examine if genetic knockdown of $\beta_2$AR similarly affected tumor cell invasive capacity, we first assessed the effect on *MMP2* expression, as a transcriptional readout of tumor cell invasion. Treatment with the βAR agonist isoproterenol increased *MMP2* expression in scramble control tumor cells (black bars, Fig. 2a), consistent with previous findings that βAR signaling regulates *MMP* expression (Yang et al., 2006), but the effect was attenuated in $\beta_2$AR knockdown cells (grey bars, Fig. 2a). Pharmacological blockade of $\beta_2$AR signaling using the $\beta_2$AR-selective antagonist ICI-118,551 abolished the effect of isoproterenol on *MMP2* expression in scramble control cells, providing pharmacological confirmation that *MMP2* expression is sensitive to $\beta_2$AR signaling (Fig. 2a). Of note, ICI-118,551 further reduced *MMP2* expression in isoproterenol-treated $\beta_2$AR-deficient cells to baseline levels (Fig. 2a), indicating that the incomplete knockdown of $\beta_2$AR (Fig. 1a) may be responsible for the residual *MMP2* expression observed in isoproterenol-treated knockdown cell lines (Fig. 2a).

To examine if $\beta_2$AR knockdown also affected tumor cell morphology, we used high-content screening to investigate the effect of $\beta_2$AR knockdown on MDA-MB-231$^{HM}$ cell morphology. Treatment of scramble control cells with the βAR agonist isoproterenol (vs. vehicle) *in vitro*, steadily increased the proportion of mesenchymal-like cells over 3 days of treatment (black line, Fig. 2b). In contrast, $\beta_2$AR knockdown attenuated the effect of isoproterenol on mesenchymal morphology at day 3 ($p < 0.001$ for shADRB2a, $p < 0.05$ for shADRB2b; grey lines, Fig. 2b and c). Additionally, pharmacological blockade of $\beta_2$AR signaling using the

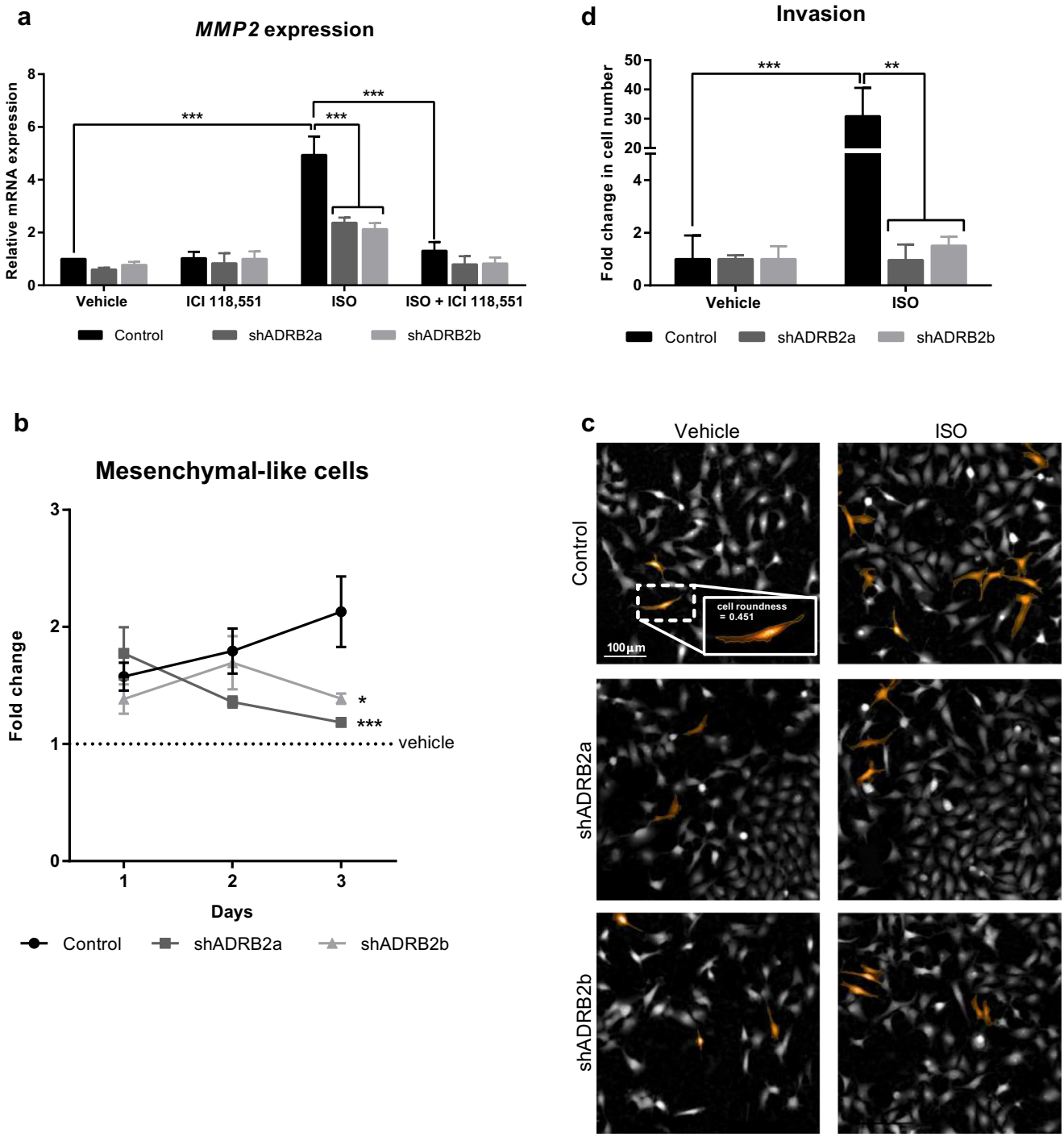


**Fig. 2. Characterization of tumor cell invasiveness in $\beta_2$AR-deficient MDA-MB-231$^{HM}$ breast cancer cells**. (a) Quantification of *MMP2* mRNA transcript levels using qRT-PCR in scramble control, shADRB2a and shADRB2b tumor cells treated with vehicle, isoproterenol (non-selective βAR agonist, ISO, 1 μM) and/or ICI-118,551 ($\beta_2$AR-selective antagonist, 1 μM) ($n$ = 3–5). (b) Fold change in proportion of tumor cells that exhibit mesenchymal-like morphology (defined by cell roundness <0.5) in response to ISO (1 μM, normalized to vehicle) ($n$ = 5–6). (c) Representative images of mesenchymal-like cells (roundness <0.5) highlighted in orange, in cultures of scramble control, shADRB2a, shADRB2b cells after treatment with vehicle or 1 μM ISO. Inset: a magnified view of a mesenchymal-like tumor cell. Scale bar: 100 μm). (d) Quantification of invasion through transwells by scramble control, shADRB2a and shADRB2b tumor cells in response to ISO (1 μM) treatment ($n$ = 4). Data represent mean ± standard error. $^{*}p < 0.05$, $^{**}p < 0.01$ and $^{***}p < 0.001$ by (b) one-way ANOVA with repeated measures or (a and d) two-way ANOVA with *post hoc* Tukey's planned comparison tests. $^{\#}p < 0.05$, $^{\#\#\#}p < 0.001$ for ISO vs. ISO + ICI-118551 within each cell line. (For interpretation of the references to colour in this figure legend, the reader is referred to the web version of this article.)

$\beta_2$AR-selective antagonist ICI-118,551 abolished the effect of isoproterenol on mesenchymal morphology in scramble control cells (Supplementary Fig. 2a and b), pharmacologically confirming a role for $\beta_2$AR in tumor cell mesenchymal morphology.

Morphological transition from epithelial-like to a mesenchymal-like phenotype has been linked with increased tumor cell invasiveness. To examine whether $\beta_2$AR knockdown also impaired the functional invasiveness of tumor cells, we treated MDA-MB-231$^{HM}$ cells with the non-selective βAR agonist isoproterenol and examined tumor cell invasion through a basement membrane using a transwell invasion assay. Isoproterenol increased invasion in scramble control cells by 30-fold ($p < 0.05$) (Fig. 2d). However, this effect of

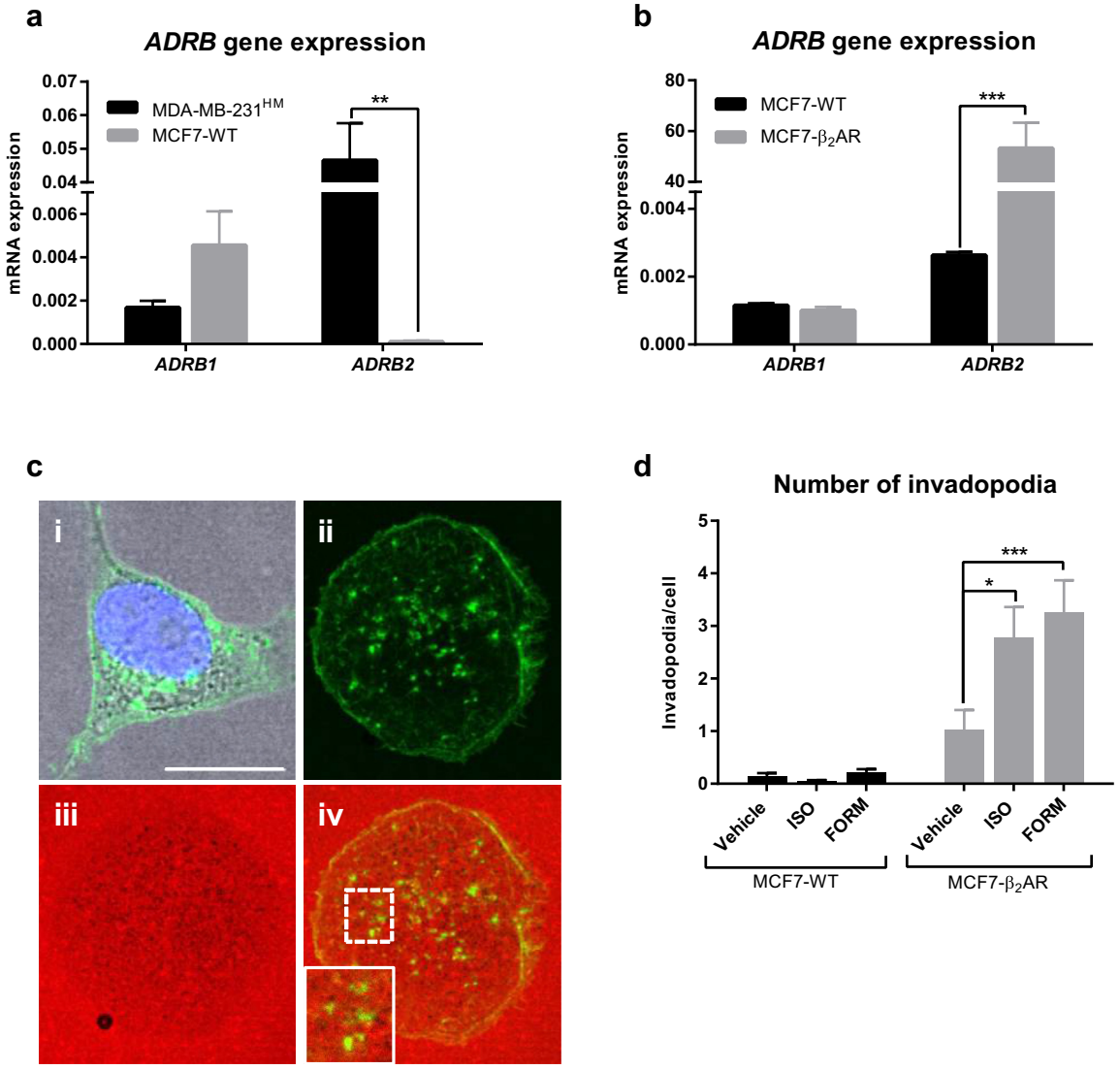


**Fig. 3. Overexpression of $\beta_2$AR in MCF-7 cells increases tumor cell invasiveness.** (a and b) Quantification of *ADRB* mRNA transcript levels using qRT-PCR in (a) MDA-MB-231$^{HM}$ and MCF-7 wildtype (MCF7-WT) cells ($n = 3$) and (b) MCF7-WT and MCF-7 overexpressing $\beta_2$AR (MCF7-$\beta_2$AR) cells ($n = 3$). Normalized to *ACTB* levels. (c) Representative images of invadopodia formation assay. Panel (i). A MCF7 cell showing $\beta_2$AR-GFP (green). Panels (ii–iv). A cell showing (ii) localization of actin foci (green), (iii) matrix degradation (grey patches of degradation on red-fluorescent gelatin), and (iv) merged image with inset panel showing active invadopodia that have degraded matrix. Scale bar: 10 μm. (d) Quantification of invadopodia per cell in MCF7-WT cells and MC7-$\beta_2$AR cells treated with vehicle, isoproterenol (non-selective βAR agonist, ISO, 0.5 μM) or formoterol ($\beta_2$AR-selective agonist, FORM, 0.5 μM) ($n > 80$ cells per condition). Data represent mean ± standard error. $^{*}p < 0.05$ and $^{***}p < 0.001$ by (a and b) unpaired *t*-tests or (d) one-way ANOVA with *post hoc* Tukey's planned comparison tests. (For interpretation of the references to colour in this figure legend, the reader is referred to the web version of this article.)

isoproterenol was abrogated in tumor cells deficient for $\beta_2$ARs (Fig. 2d), confirming that $\beta_2$AR signaling in MDA-MB-231$^{HM}$ tumor cells drives invasion. Collectively, these findings confirm that genetic knockdown of $\beta_2$AR modulates the tumor cell invasive phenotype in a way that replicates pharmacological $\beta_2$AR blockade (Creed et al., 2015; Pon et al., 2016).

MMPs are localized at subcellular structures called invadopodia that regulate invasion of tumor cells (Murphy and Courtneidge, 2011). We found previously that $\beta_2$AR regulation of invasion is mediated by formation of invadopodia (Creed et al., 2015). To independently validate the findings that genetic modulation of $\beta_2$AR affects tumor cell invasion, we overexpressed $\beta_2$AR in MCF-7 breast cancer cells which have low endogenous levels of $\beta_2$AR, compared to MDA-MB-231$^{HM}$ cells (Fig. 3a), and investigated the effect on formation of invadopodia. MCF-7 cells were transduced with a construct encoding a $\beta_2$AR-GFP fusion protein and $\beta_2$AR overexpression was confirmed at both the transcript and protein level using qRT-PCR and fluorescence microscopy, respectively (Fig. 3b and c). Tumor cell invasive capacity was assessed by formation of invasive invadopodia structures that degrade underlying extracellular matrix (Fig. 3c). Treatment with the $\beta_2$AR-selective agonist formoterol or the non-selective agonist isoproterenol induced formation of invadopodia in cells that overexpressed $\beta_2$AR, but not in wildtype MCF-7 cells (Fig. 3d). Collectively, these *in vitro* findings confirm that genetically modulating $\beta_2$AR by either overexpression or knockdown, affects isoproterenol-induced tumor cell invasiveness, as demonstrated by transcriptional, morphological and functional readouts (Figs. 2 and 3).

### 3.3. $\beta_2$AR-driven tumor cell invasion contributes to stress-enhanced metastasis in vivo

Having established that knockdown of $\beta_2$AR in MDA-MB-231$^{HM}$ cells limits βAR-regulated invasion *in vitro* (Fig. 2d) without

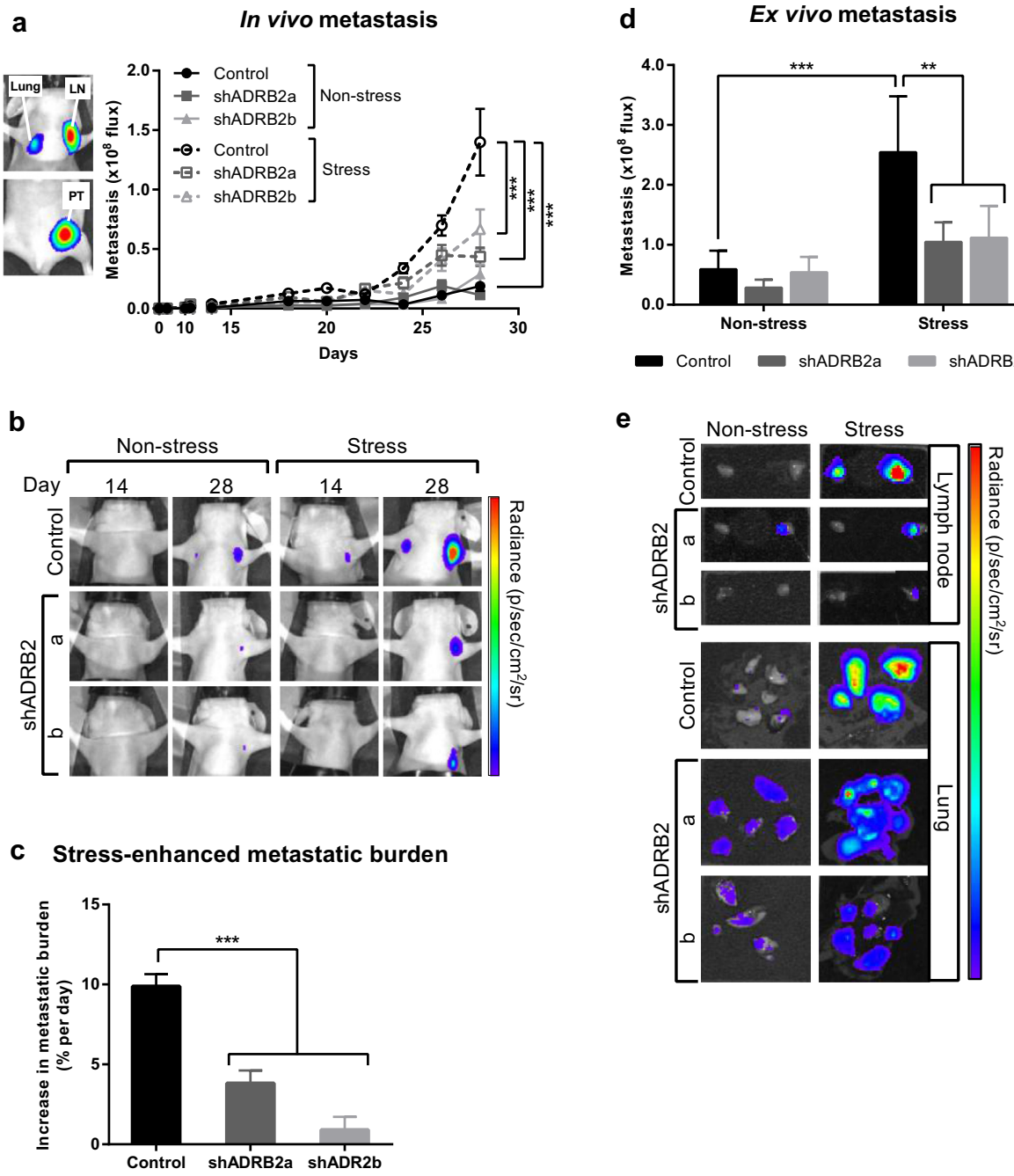


**Fig. 4. $\beta_2$AR knockdown in MDA-MB-231$^{HM}$ breast cancer cells impairs metastasis *in vivo*.** (a) Left panel: representative *in vivo* bioluminescence image of the orthotopic MDA-MB-231$^{HM}$ breast cancer model showing primary tumor (PT) and spontaneously disseminated metastasis in lymph node (LN) and lung 28 days after tumor cell injection. Right panel: quantification of distant metastasis by bioluminescence imaging in mice with tumors derived from scramble control or $\beta_2$AR-deficient cells (shADRB2a and shADRB2b). Mice were exposed to non-stress or stress conditions. ($n = 5$ at each time point). (b) Representative images of metastasis *in vivo* at day 14 and 28 after tumor cell injection. Note: the primary tumor is not visible. Scale: min. $3 \times 10^6$ photons/s; max. $1 \times 10^8$ photons/s. (c) The magnitude of the effect of stress on metastatic burden was computed as the difference in the rate of metastatic progression under non-stress and stress conditions. (d) *Ex vivo* quantification of distant metastasis in target organs that were harvested from mice 28 days after tumor cell injection ($n = 5$). (e) Representative images of metastasis in lung and lymph node *ex vivo* at 28 days post tumor cell inoculation. Scale: lymph node: min. $5 \times 10^6$; max. $1 \times 10^8$ and lung: min. $2 \times 10^5$; max. $8 \times 10^6$ photons/s. Data represent mean ± standard error. $^*p < 0.05$ and $^{***}p < 0.001$ by (c) one-way ANOVA or two-way ANOVA (a) with or (d) without repeated measures followed by *post hoc* Tukey's planned comparison tests.

compromising proliferation (Fig. 1c), we investigated whether knockdown of $\beta_2$AR in tumor cells also modulates the effect of stress on metastatic dissemination from a primary tumor *in vivo*. In the complex environment of the tumor, many stromal cell populations can also respond to $\beta_2$AR signaling, which plausibly may offset the effect of $\beta_2$AR-knockdown in tumor cells on metastasis. To model breast cancer, scramble control tumor cells or $\beta_2$AR knockdown tumor cells were injected into the mammary fat pad of mice and bioluminescence imaging was used to non-invasively quantify the onset and kinetics of metastasis to distant organs (Fig. 4a). Longitudinal analysis of spontaneous dissemination of metastatic tumor cells from the primary tumor found that under baseline (non-stress) conditions, knockdown of $\beta_2$AR had no effect on metastasis (Fig. 4a solid lines, and b). By day 28 of tumor progression, in mice with tumors derived from scramble control tumor cells, chronic restraint stress increased metastasis by 10-fold,

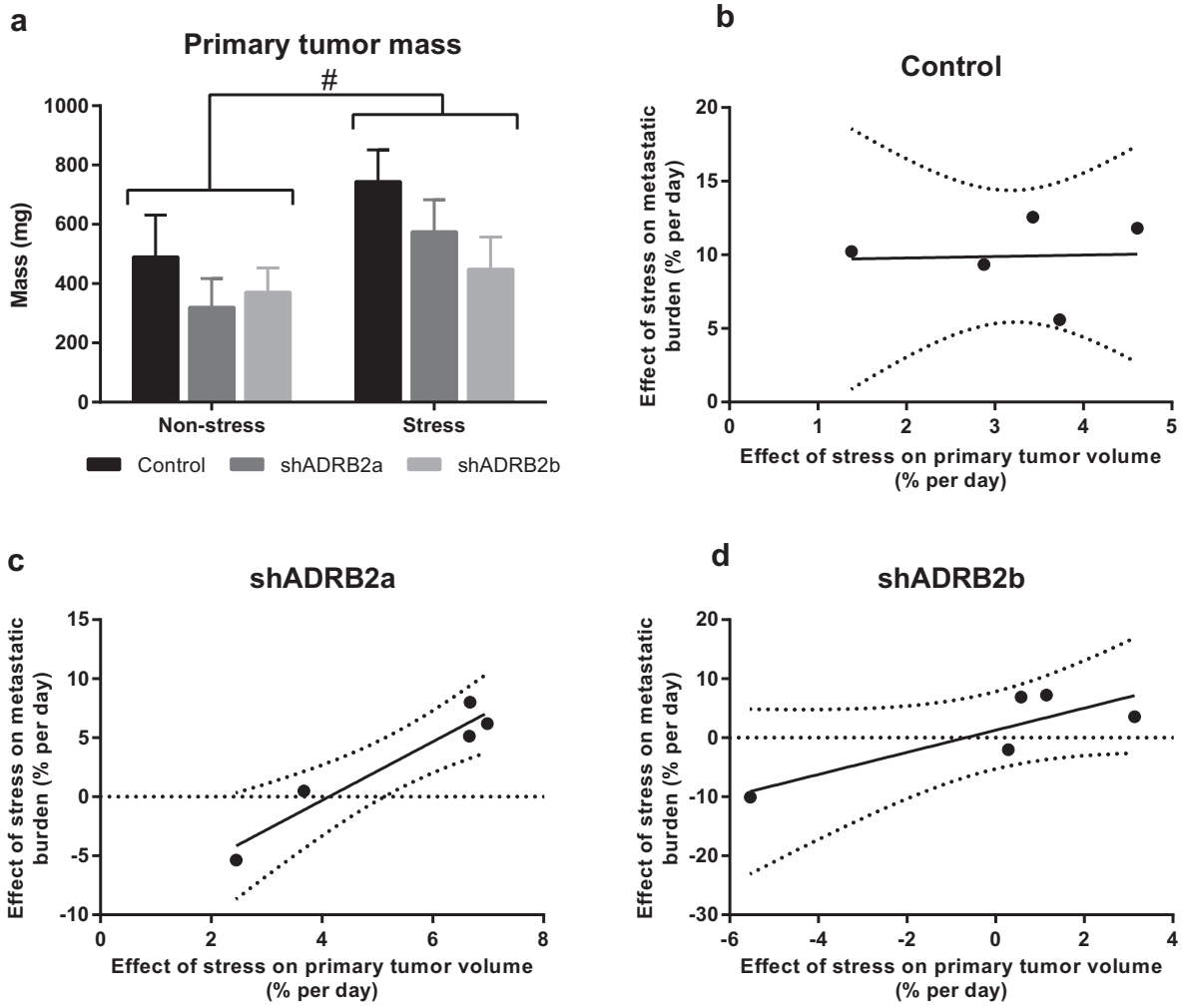


**Fig. 5. Stress-enhanced metastasis is independent of primary tumor size.** (a) Mass of tumors derived from control or $\beta_2$AR-deficient cells, from mice exposed to non-stress or stress conditions ($n = 5$). (b–d) Pearson correlation analysis of the relationship between the effect of stress on the trajectory of metastasis and the effect of stress on the trajectory of primary tumor growth in mice bearing (b) control ($r^2 = 0.001938$, $p = 0.944$), (c) shADRB2a ($r^2 = 0.9224$, $p = 0.0094$), and (d) shADRB2b ($r^2 = 0.6995$, $p = 0.0775$) tumors. $^{\#}p < 0.05$ for main stress effect by two-way ANOVA.

compared to non-stress conditions (Fig. 4a), consistent with previous findings (Lamkin et al., 2015; Le et al., 2016; Sloan et al., 2010). This overall increase in metastasis occurred as a consequence of a daily 9.9% ± 0.77% increase in metastatic burden for the duration of the experiment (Fig. 4c). Significantly, knockdown of *ADRB2* in tumor cells reduced this cumulative effect of stress on metastasis, with mice bearing shADRB2a or shADRB2b tumors displaying a reduction in stress-enhanced metastasis by 61.41% ± 12.25% ($p < 0.001$) and 85.86% ± 13.30% ($p < 0.001$) respectively, compared to mice with scramble control tumors (Fig. 4a–c).

To evaluate the effect of $\beta_2$AR knockdown on tumor burden in metastatic target organs, we used *ex vivo* bioluminescence imaging to quantify metastatic tumor cells that had spread from the primary mammary tumor to lymph node and lung. *Ex vivo* analysis confirmed that $\beta_2$AR knockdown in MDA-MB-231$^{HM}$ tumor cells blocked stress from increasing metastasis to both lymph node and lung ($p = 0.001$, versus scramble control tumor cells) (Fig. 4d and e).

The rate of primary tumor growth is highly prognostic for the extent of tumor cell spread (Weigelt et al., 2005). Therefore, the effects of $\beta_2$AR signaling on metastasis may have occurred secondary to the effects on the primary tumor. In fact, assessment of primary tumor mass on day 28 of tumor growth revealed that stress produced a small, but significant, increase in primary tumor growth regardless of the $\beta_2$AR status of tumors ($p < 0.05$; Fig. 5a). We used regression analysis to evaluate the relationship between the effect of stress on primary tumor growth rate and the effect of stress on metastasis. Interestingly, the effect of stress on the primary tumor did not predict the effect of stress on metastasis in control tumor cells with intact $\beta_2$AR signaling (Fig. 5b). However, knockdown of $\beta_2$AR resulted in the expected positive correlation between primary tumor growth rate and trajectory of metastatic burden (Fig. 5c and d). Therefore, when $\beta_2$AR is present on tumor cells, stress drives metastasis independently of primary tumor growth. Collectively, these findings demonstrate that even in the complex tumor microenvironment where multiple cell populations may respond to βAR signaling, $\beta_2$AR-driven tumor cell invasion significantly contributes to the effects of stress on accelerating metastasis. Furthermore, these findings demonstrate the feasibility of targeting $\beta_2$AR-driven tumor cell invasion to inhibit the adverse effects of stress on breast cancer metastasis.

## 4. Discussion

Despite major advances in cancer treatment, metastasis remains a significant clinical challenge in the breast cancer clinic. We and others have shown that chronic stress acts through βAR signaling to drive metastasis (Kim-Fuchs et al., 2014; Le et al.,

2016; Liu et al., 2015; Sloan et al., 2010; Thaker et al., 2006; Zhao et al., 2015), and our previous *in vitro* findings have demonstrated that $\beta_2$AR signaling in cancer cells enhances invadopodia formation and promotes tumor cell invasion *in vitro* (Creed et al., 2015; Pon et al., 2016). However, the contribution of direct activation of $\beta_2$AR signaling in tumor cells (rather than through effects on the tumor stroma) to metastatic dissemination from a primary tumor is unclear. Here, we extend our understanding by showing that $\beta_2$AR signaling in human MDA-MB-231$^{HM}$ breast cancer cells contributes to the deleterious effects of stress on metastatic dissemination from the complex microenvironment of a primary mammary tumor. We found that silencing $\beta_2$AR expression in MDA-MB-231$^{HM}$ breast cancer cells blocked the effect of stress on metastasis *in vivo*, which identifies tumor cells as an additional *in vivo* target of stress-induced βAR signaling. These results expand on earlier findings that demonstrated a role for stromal cells in the tumor microenvironment in the adverse effects of stress on metastasis, and suggests that βAR signaling in both tumor cells and stromal cells contributes to the effect of stress on metastasis. This raises the possibility that inhibiting stress signaling to either tumor cells (as shown here) or to the tumor stroma (Le et al., 2016; Sloan et al., 2010) may be sufficient to modulate metastasis.

Invasion is one of the critical steps along the metastatic cascade that determines successful metastatic outgrowth. Notably, incomplete knockdown of $\beta_2$AR in MDA-MB-231$^{HM}$ tumor cells (Fig. 1a) was sufficient to diminish stress-enhanced metastasis (Fig. 4a and c), suggesting that even partial modulation of tumor cell $\beta_2$AR may be sufficient to slow breast cancer progression. We also showed that the effects of stress-induced tumor $\beta_2$AR signaling on metastasis was independent of the effect on primary tumor size (Fig. 5b–d). These results extend our previous findings that pharmacological modulation of tumor cell $\beta_2$AR regulates tumor cell invasion *in vitro* (Creed et al., 2015; Pon et al., 2016), by showing that $\beta_2$AR signaling in tumor cells also plays a key role in driving metastasis *in vivo*.

It is possible that $\beta_2$AR signaling may regulate an epithelial-to-mesenchymal transition in tumor cells to increase metastatic invasion and dissemination. Here, we observed that isoproterenol treatment shifted MDA-MB-231$^{HM}$ cells towards a mesenchymal morphology (Fig 2a), an effect that was attenuated by $\beta_2$AR knockdown. It will be important to characterize if $\beta_2$AR agonism induces similar behavior in other tumor cell lines and *in vivo*. Notably, several recent *in vitro* studies suggest that βAR signaling induces an epithelial-mesenchymal transition in gastric, colon and lung cancer cell lines (Lu et al., 2015; Shan et al., 2014; Zhang et al., 2016). To better understand βAR regulation of epithelial-mesenchymal transition it will be necessary to clarify the molecular mechanisms. While we found no evidence that βAR signaling regulates expression of the mesenchymal marker vimentin in MDA-MB-231$^{HM}$ breast cancer cells (data not shown), it will be important to evaluate other molecules that are known to influence epithelial-mesenchymal transition, including SNAIL and TWIST1. Such studies should control for catecholamine-induced autooxidation, which may also induce morphological changes.

While the *in vivo* findings described here are limited to the contribution of tumor cell $\beta_2$AR in metastatic dissemination in the MDA-MB-231$^{HM}$ model of breast cancer, findings that stress also increases metastasis in models of ovarian cancer (Thaker et al., 2006), pancreatic cancer (Kim-Fuchs et al., 2014), and colorectal cancer (Liu et al., 2015; Zhao et al., 2015), suggest that it will be important to examine the role of tumor cell $\beta_2$AR in metastatic dissemination of other tumor types. Additionally, while these results highlight βAR-regulated tumor cell invasion as a significant contributor to cancer progression, they do not exclude a role for βAR signaling to stromal cells in the adverse effects of stress on metastasis (Le et al., 2016; Sloan et al., 2010; Thaker et al., 2006). It is likely that the beneficial effects of βAR-targeted therapies (e.g., β-blockers) on slowing metastasis are due to effects on both tumor cells and stromal cells. Myeloid cells are sensitive to βAR signaling (Le et al., 2016; Powell et al., 2013), which leads to their accumulation in primary tumors where they remodel blood and lymphatic vasculature to provide additional routes for tumor cell dissemination (Le et al., 2016; Sloan et al., 2010; Thaker et al., 2006). To fully characterize the interactions between tumor cells and stromal cells that mediate the effects of stress on metastasis, it will be valuable to use additional strategies including *ADRB2* knockout mice and cell-specific *ADRB2* deletion mutants to probe the contributions of various cell types in the tumor microenvironment to stress-induced cancer progression.

There are three subtypes of βAR that are expressed on both stroma cells and tumor cells (Badino et al., 1996; Du et al., 2014; Reeder et al., 2015; Vandewalle et al., 1990). While $\beta_2$AR is the only functional βAR subtype in MDA-MB-231$^{HM}$ cells (Creed et al., 2015; Pon et al., 2016), other cancer cells have been shown to express $\beta_1$AR and $\beta_3$AR subtypes (Dal Monte et al., 2013; Kim-Fuchs et al., 2014; Magnon et al., 2013). However, the role of these receptor subtypes in cancer progression is only starting to be elucidated (Magnon et al., 2013). As the use of β-blockers to slow metastasis is clinically translated, it will be important to investigate the role of other βAR subtypes in cancer progression. Second generation β-blockers were developed for increased cardio-specificity by increasing their selectivity for $\beta_1$ARs, and are now more commonly used than older generation non-selective β-blockers (Salpeter, 2003). Our findings that $\beta_2$ARs on MDA-MB-231$^{HM}$ tumor cells also contribute to metastasis suggest that some breast cancers may be more effectively targeted with antagonists that also inhibit $\beta_2$ARs (e.g., propranolol). This is supported by a recent retrospective epidemiological study that found the use of non-selective β-blockers that target both $\beta_1$AR and $\beta_2$AR, but not $\beta_1$AR-selective blockers, was associated with improved cancer outcome (Barron et al., 2011). These findings provide insights into the contribution of tumor cell $\beta_2$AR signaling in stress-enhanced cancer progression and further support the use of β-blockers to modulate breast cancer metastasis.

## Conflict of interest

The authors declare that they have no conflict of interest.

## Contributions

Aeson Chang and Caroline P. Le designed and conducted experiments, analyzed data, and wrote the manuscript. Adam K. Walker interpreted data and wrote the manuscript. Sarah J. Creed conducted *in vitro* experiments. Cindy K. Pon conducted cAMP experiments. Sabine Albold generated knockdown cell lines. Dominic Carroll conducted *in vivo* experiments. Michelle L. Halls, J. Robert Lane, Bernhard Riedel and Davide Ferrari analyzed data. Erica K. Sloan designed the study, conducted experiments, analyzed data and wrote the manuscript. All authors reviewed the manuscript.

## Acknowledgments

The authors thank Dr. Kaylene Simpson from the Victorian Centre for Functional Genomics at Peter MacCallum Cancer Center for assistance with shRNA techniques, Dr. Bronwyn Evans from Monash University for the $\beta_2$AR-GFP construct, and the Imaging, Flow Cytometry and Analysis Core at Monash Institute of Pharmaceutical Sciences for imaging and data analysis support. This research was supported by the Australian National Health and Medical

Research Council (1008865), the Australian Research Council (LE110100125), the National Cancer Institute (CA160890), a National Breast Cancer Foundation fellowship to Adam K. Walker (PF-15-014), a National Health and Medical Research Council RD Wright Fellowship to Michelle L. Halls (1061687), Monash Institute of Pharmaceutical Sciences-Drug Discovery Biology (MIPS-DDB) Strategic Funding, the David Skewes Foundation and the Peter MacCallum Cancer Foundation.

## Appendix A. Supplementary data

Supplementary data associated with this article can be found, in the online version, at http://dx.doi.org/10.1016/j.bbi.2016.06.011.

## References

Abrass, C.K., O'Connor, S.W., Scarpace, P.J., Abrass, I.B., 1985. Characterization of the beta-adrenergic receptor of the rat peritoneal macrophage. J. Immunol. 135, 1338–1341.
Badino, G.R., Novelli, A., Girardi, C., Di Carlo, F., 1996. Evidence for functional beta-adrenoceptor subtypes in CG-5 breast cancer cell. Pharmacol. Res. 33, 255–260.
Barron, T.I., Connolly, R.M., Sharp, L., Bennett, K., Visvanathan, K., 2011. Beta blockers and breast cancer mortality: a population-based study. J. Clin. Oncol. 29, 2635–2644.
Ben-Eliyahu, S., Shakhar, G., Page, G.G., Stefanski, V., Shakhar, K., 2000. Suppression of NK cell activity and of resistance to metastasis by stress: a role for adrenal catecholamines and beta-adrenoceptors. NeuroImmunoModulation 8, 154–164.
Bissell, M.J., Labarge, M.A., 2005. Context, tissue plasticity, and cancer: are tumor stem cells also regulated by the microenvironment? Cancer Cell 7, 17–23.
Bretz, F., Hothorn, T., Westfall, P., 2010. Multiple Comparisons Using R. CRC Press.
Campbell, J.P., Karolak, M.R., Ma, Y., Perrien, D.S., Masood-Campbell, S.K., Penner, N. L., Munoz, S.A., Zijlstra, A., Yang, X., Sterling, J.A., Elefteriou, F., 2012. Stimulation of host bone marrow stromal cells by sympathetic nerves promotes breast cancer bone metastasis in mice. PLoS Biol. 10, e1001363.
Chang, X.Z., Li, D.Q., Hou, Y.F., Wu, J., Lu, J.S., Di, G.H., Jin, W., Ou, Z.L., Shen, Z.Z., Shao, Z.M., 2008. Identification of the functional role of AF1Q in the progression of breast cancer. Breast Cancer Res. Treat. 111, 65–78.
Condeelis, J., Pollard, J.W., 2006. Macrophages: obligate partners for tumor cell migration, invasion, and metastasis. Cell 124, 263–266.
Creed, S.J., Le, C.P., Hassan, M., Pon, C.K., Albold, S., Chan, K.T., Berginski, M.E., Huang, Z., Bear, J.E., Lane, J.R., Halls, M.L., Ferrari, D., Nowell, C.J., Sloan, E.K., 2015. Beta2-adrenoceptor signaling regulates invadopodia formation to enhance tumor cell invasion. Breast Cancer Res. BCR 17, 145.
Dal Monte, M., Casini, G., Filippi, L., Nicchia, G.P., Svelto, M., Bagnoli, P., 2013. Functional involvement of beta3-adrenergic receptors in melanoma growth and vascularization. J. Mol. Med. 91, 1407–1419.
Devaud, C., Westwood, J.A., John, L.B., Flynn, J.K., Paquet-Fifield, S., Duong, C.P., Yong, C.S., Pegram, H.J., Stacker, S.A., Achen, M.G., Stewart, T.J., Snyder, L.A., Teng, M. W., Smyth, M.J., Darcy, P.K., Kershaw, M.H., 2014. Tissues in different anatomical sites can sculpt and vary the tumor microenvironment to affect responses to therapy. Mol. Ther. 22, 18–27.
Du, Y., Zhou, L., Wang, Y., Yan, T., Jiang, Y., Shao, Z., Yin, W., Lu, J., 2014. Association of alpha2a and beta2 adrenoceptor expression with clinical outcome in breast cancer. Curr. Med. Res. Opin. 30, 1337–1344.
Elenkov, I.J., Wilder, R.L., Chrousos, G.P., Vizi, E.S., 2000. The sympathetic nerve–an integrative interface between two supersystems: the brain and the immune system. Pharmacol. Rev. 52, 595–638.
Folkman, J., 2002. Role of angiogenesis in tumor growth and metastasis. Semin. Oncol. 29, 15–18.
Graf, K., Grafe, M., Dummler, U., O'Connor, A., Regitz-Zagrosek, V., Kunkel, G., Auch-Schwelk, W., Fleck, E., 1993. Regulation of beta-adrenergic receptors on endothelial cells in culture. Eur. Heart J. 14 (Suppl. I), 173–176.
Kim-Fuchs, C., Le, C.P., Pimentel, M.A., Shackleford, D., Ferrari, D., Angst, E., Hollande, F., Sloan, E.K., 2014. Chronic stress accelerates pancreatic cancer growth and invasion: a critical role for beta-adrenergic signaling in the pancreatic microenvironment. Brain Behav. Immun. 40, 40–47.
Lamkin, D., Sung, H., Yang, G., David, J., Ma, J., Cole, S., 2015. Alpha2-adrenergic blockade mimics the enhancing effect of chronic stress on breast cancer progression. Psychoneuroendocrinology 51, 262–270.
Le, C.P., Nowell, C.J., Kim-Fuchs, C., Botteri, E., Hiller, J.G., Ismail, H., Pimentel, M.A., Chai, M.G., Karnezis, T., Rotmensz, N., Renne, G., Gandini, S., Pouton, C.W., Ferrari, D., Moller, A., Stacker, S.A., Sloan, E.K., 2016. Chronic stress in mice remodels lymph vasculature to promote tumour cell dissemination. Nat. Commun. 7, 10634.
Liu, J., Deng, G.H., Zhang, J., Wang, Y., Xia, X.Y., Luo, X.M., Deng, Y.T., He, S.S., Mao, Y. Y., Peng, X.C., Wei, Y.Q., Jiang, Y., 2015. The effect of chronic stress on anti-angiogenesis of sunitinib in colorectal cancer models. Psychoneuroendocrinology 52, 130–142.
Lu, Y.J., Geng, Z.J., Sun, X.Y., Li, Y.H., Fu, X.B., Zhao, X.Y., Wei, B., 2015. Isoprenaline induces epithelial-mesenchymal transition in gastric cancer cells. Mol. Cell. Biochem. 408, 1–13.
Magnon, C., Hall, S.J., Lin, J., Xue, X., Gerber, L., Freedland, S.J., Frenette, P.S., 2013. Autonomic nerve development contributes to prostate cancer progression. Science 341, 1236361.
Mehlen, P., Puisieux, A., 2006. Metastasis: a question of life or death. Nat. Rev. Cancer 6, 449–458.
Murphy, D.A., Courtneidge, S.A., 2011. The 'ins' and 'outs' of podosomes and invadopodia: characteristics, formation and function. Nat. Rev. Mol. Cell Biol. 12, 413–426.
Pon, C.K., Lane, J.R., Sloan, E.K., Halls, M.L., 2016. The beta2-adrenoceptor activates a positive cAMP-calcium feedforward loop to drive breast cancer cell invasion. FASEB J. 30, 1144–1154.
Powell, N.D., Sloan, E.K., Bailey, M.T., Arevalo, J.M., Miller, G.E., Chen, E., Kobor, M.S., Reader, B.F., Sheridan, J.F., Cole, S.W., 2013. Social stress up-regulates inflammatory gene expression in the leukocyte transcriptome via beta-adrenergic induction of myelopoiesis. Proc. Natl. Acad. Sci. U.S.A. 110, 16574–16579.
Reeder, A., Attar, M., Nazario, L., Bathula, C., Zhang, A., Hochbaum, D., Roy, E., Cooper, K.L., Oesterreich, S., Davidson, N.E., Neumann, C.A., Flint, M.S., 2015. Stress hormones reduce the efficacy of paclitaxel in triple negative breast cancer through induction of DNA damage. Br. J. Cancer 112, 1461–1470.
Ren, Z.X., Yu, H.B., Li, J.S., Shen, J.L., Du, W.S., 2015. Suitable parameter choice on quantitative morphology of A549 cell in epithelial-mesenchymal transition. Biosci. Rep. 35.
Salpeter, S.R., 2003. Cardioselective beta blocker use in patients with asthma and chronic obstructive pulmonary disease: an evidence-based approach to standards of care. Cardiovasc. Rev. Rep. 24, 1.
Sanders, V.M., Baker, R.A., Ramer-Quinn, D.S., Kasprowicz, D.J., Fuchs, B.A., Street, N. E., 1997. Differential expression of the beta2-adrenergic receptor by Th1 and Th2 clones: implications for cytokine production and B cell help. J. Immunol. 158, 4200–4210.
Schindelin, J., Arganda-Carreras, I., Frise, E., Kaynig, V., Longair, M., Pietzsch, T., Preibisch, S., Rueden, C., Saalfeld, S., Schmid, B., Tinevez, J.Y., White, D.J., Hartenstein, V., Eliceiri, K., Tomancak, P., Cardona, A., 2012. Fiji: an open-source platform for biological-image analysis. Nat. Methods 9, 676–682.
Shan, T., Cui, X., Li, W., Lin, W., Li, Y., Chen, X., Wu, T., 2014. Novel regulatory program for norepinephrine-induced epithelial-mesenchymal transition in gastric adenocarcinoma cell lines. Cancer Sci. 105, 847–856.
Sloan, E.K., Priceman, S.J., Cox, B.F., Yu, S., Pimentel, M.A., Tangkanangnukul, V., Arevalo, J.M., Morizono, K., Karanikolas, B.D., Wu, L., Sood, A.K., Cole, S.W., 2010. The sympathetic nervous system induces a metastatic switch in primary breast cancer. Cancer Res. 70, 7042–7052.
Thaker, P.H., Han, L.Y., Kamat, A.A., Arevalo, J.M., Takahashi, R., Lu, C., Jennings, N.B., Armaiz-Pena, G., Bankson, J.A., Ravoori, M., Merritt, W.M., Lin, Y.G., Mangala, L. S., Kim, T.J., Coleman, R.L., Landen, C.N., Li, Y., Felix, E., Sanguino, A.M., Newman, R.A., Lloyd, M., Gershenson, D.M., Kundra, V., Lopez-Berestein, G., Lutgendorf, S. K., Cole, S.W., Sood, A.K., 2006. Chronic stress promotes tumor growth and angiogenesis in a mouse model of ovarian carcinoma. Nat. Med. 12, 939–944.
Vandewalle, B., Revillion, F., Lefebvre, J., 1990. Functional beta-adrenergic receptors in breast cancer cells. J. Cancer Res. Clin. Oncol. 116, 303–306.
Verbeke, G., Molenberghs, G., 2009. Linear Mixed Models for Longitudinal Data. Springer, New York.
Weigelt, B., Peterse, J.L., van't Veer, L.J., 2005. Breast cancer metastasis: markers and models. Nat. Rev. Cancer 5, 591–602.
Yamazaki, S., Miyoshi, N., Kawabata, K., Yasuda, M., Shimoi, K., 2014. Quercetin-3-O-glucuronide inhibits noradrenaline-promoted invasion of MDA-MB-231 human breast cancer cells by blocking beta(2)-adrenergic signaling. Arch. Biochem. Biophys. 557, 18–27.
Yang, J., Weinberg, R.A., 2008. Epithelial-mesenchymal transition: at the crossroads of development and tumor metastasis. Dev. Cell 14, 818–829.
Yang, E.V., Sood, A.K., Chen, M., Li, Y., Eubank, T.D., Marsh, C.B., Jewell, S., Flavahan, N.A., Morrison, C., Yeh, P.E., Lemeshow, S., Glaser, R., 2006. Norepinephrine up-regulates the expression of vascular endothelial growth factor, matrix metalloproteinase (MMP)-2, and MMP-9 in nasopharyngeal carcinoma tumor cells. Cancer Res. 66, 10357–10364.
Zhang, J., Deng, Y.T., Liu, J., Wang, Y.Q., Yi, T.W., Huang, B.Y., He, S.S., Zheng, B., Jiang, Y., 2016. Norepinephrine induced epithelial-mesenchymal transition in HT-29 and A549 cells in vitro. J. Cancer Res. Clin. Oncol. 142, 423–435.
Zhao, L., Xu, J., Liang, F., Li, A., Zhang, Y., Sun, J., 2015. Effect of chronic psychological stress on liver metastasis of colon cancer in mice. PLoS One 10, e0139978.